Functional Morphometry of Horizontal Rectus Extraocular Muscles during Horizontal Ocular Duction

Robert A. Clark[1] *and Joseph L. Demer*[1–4]

Purpose. We explored multiple quantitative measures of horizontal rectus extraocular muscle (EOM) morphology to determine the magnetic resonance imaging (MRI) measure best correlating with duction and thus contractility.

Methods. Surface coil coronal MRI was obtained in target-controlled central gaze and multiple positions of adduction and abduction in 26 orbits of 15 normal volunteers. Duction angles were determined by position changes of the globe-optic nerve junction. Cross-sectional areas, partial volumes, and location of peak cross-sections of the horizontal rectus EOMs were computed in contiguous image planes 2-mm thick spanning the EOM origins to the globe equator.

Results. All measures correlated significantly with duction angle ($P < 0.0001$). The best measures obtainable in single image planes were the maximum change in the cross-sectional area between equivalent image planes, with coefficients of determination $R^2 = 0.92$ for medial rectus (MR) and 0.91 for lateral rectus (LR), and percentage change in maximum cross-section with $R^2 = 0.79$ for MR and 0.78 for LR. The best partial volume measure of contractility was the change in partial volumes in four contiguous posterior planes ($R^2 = 0.86$ MR and for 0.89 LR), particularly when combined with the corresponding change in partial volume for the antagonist EOM ($R^2 = 0.95$ for MR and LR).

Conclusions. EOM morphologic changes are highly correlated with degrees of duction and thus contractility. Both changes in single-plane maximum cross-sectional areas and posterior partial volumes provide accurate, quantitative measures of EOM contractility. (*Invest Ophthalmol Vis Sci.* 2012;53:7375–7379) DOI:10.1167/iovs.12-9730

Magnetic resonance imaging (MRI) has consistently demonstrated substantial changes in extraocular muscle (EOM) morphology during changes in ocular duction.[1–4] For a normal EOM, the maximum cross-sectional area increases and the plane of maximum cross-sectional area shifts posteriorly during duction into that EOM's field of action, correlating with EOM contraction. In an analogous fashion, the maximum cross-sectional area diminishes and the plane of maximum cross-section shifts anteriorly during duction away from that EOM's field of action, correlating with EOM relaxation. These changes are diminished or ablated in paretic EOMs, characterized by a marked reduction in maximum cross-sectional area in central gaze and minimal changes in morphology during attempted duction into the paretic field of action.[5–8]

While these large changes in EOM morphology are sufficient to detect gross dysfunctions such as fibrosis or paralysis, they may not be sufficiently sensitive to detect more subtle abnormalities of EOM function, such as putative EOM "overaction" or "underaction,"[9,10] or contraction of only a portion of the EOM as may occur during Duane syndrome or other more complex forms of strabismus.[6,11,12] Other measures of EOM morphology, such as changes in EOM volumes in the midorbital regions, have been advocated to detect these more subtle contractile changes,[13,14] but these measures have not been validated through determination of strong correlations with EOM contractility. In this study, we examine multiple morphometric parameters of the horizontal rectus EOMs in normal subjects over a wide range of horizontal duction to determine which measurements have the strongest correlation with degrees of duction, and by inference, functional contractility.

Methods

Fifteen normal, orthotropic paid volunteer adult subjects were recruited by advertisement. A comprehensive eye examination verified normal acuity, normal ocular motility, stereoacuity, and ocular anatomy in each subject. Each subject also gave written informed consent according to a protocol conforming to the Declaration of Helsinki and approved by the Human Subject Protection Committee at the University of California, Los Angeles.

High-resolution, T2 fast spin echo MRI was performed using a 1.5-T scanner (Signa; General Electric, Milwaukee, WI) utilizing techniques described in detail elsewhere,[14,15] including use of a dual-phased surface coil array (Medical Advances, Milwaukee, WI) to improve signal-to-noise ratio and fixation targets to avoid motion artifacts. Subjects were scanned in the supine position with the head stabilized with foam cushions. During imaging, subjects fixated the end of a fiber-optic cable illuminated from its distal end by a red, light-emitting diode in central gaze and various positions of abduction and adduction at a distance of 2 cm. The target was afocal and visible to only one eye, so accommodation and binocular convergence on it was impossible, as verified by axial MRI. Targets were placed in central position for the scanned eye, as well as in slight, moderate, and maximal adduction and abduction.

Initially, a true axial image including both orbits was obtained at 3-mm thickness with a 390- to 469-micron in-plane resolution. This true axial image was used to place sets of 18 to 20 contiguous, 2-mm–thick quasicoronal images in a plane perpendicular to the long axis of each orbit using a 256 × 256 matrix over an 8-cm field of view, yielding a final pixel resolution of 312 microns. The scanned eye was imaged in maximal adduction during fixation by the fellow eye, since the nasal

From the Departments of [1]Ophthalmology, [2]Neurology, [3]Neuroscience, and [4]Biomedical Engineering Interdepartmental Programs, David Geffen Medical School, University of California, Los Angeles, California.

Supported by NEI Grant EY08313, the Shaw Family Endowment Fund, and by Research to Prevent Blindness (New York, New York). The authors alone are responsible for the content and writing of the paper.

Submitted for publication February 20, 2012; revised June 18 and September 14, 2012; accepted September 17, 2012.

Disclosure: **R.A. Clark**, None; **J.L. Demer**, None

Corresponding author: Joseph L. Demer, Jules Stein Eye Institute, 100 Stein Plaza, UCLA, Los Angeles, CA 90095-7002; jld@ucla.edu.

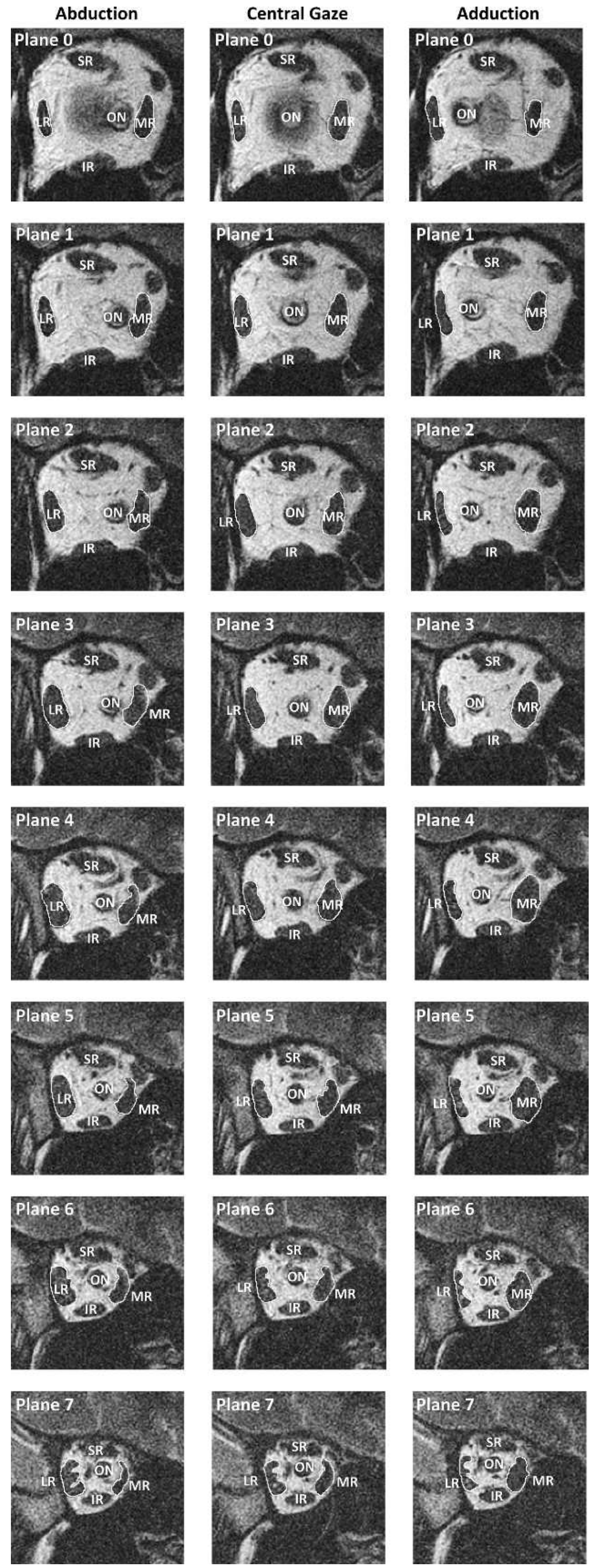

FIGURE 1. Quasi-coronal magnetic resonance images at 2-mm spacing contiguously from the globe-optic nerve junction (plane 0) to the image plane 14 mm posterior (plane 7) in abduction, central gaze, and adduction. The change in position of the globe-optic nerve junction in plane 0 was used to measure globe rotation in eccentric gaze. Cross-sectional areas were measured by manually outlining the EOM bellies (*white lines*), counting pixels within those EOMs, and converting the pixels into mm^2. Multiplane partial volume measurements were obtained by multiplying those cross-sectional areas by the slice thickness and summing partial volumes from adjacent image planes. The midorbital partial volume was measured using planes 0 to 5 and the posterior partial volume planes 4 to 7. Other partial volume measurements were posterior by two, three, or four image planes from the image plane containing the maximum cross-sectional area in central gaze, plane 2 for the LR and plane 3 for the MR for this subject. IR, inferior rectus; ON, optic nerve; SR, superior rectus.

bridge or the surface coil array in this gaze direction occluded the scanned eye.

A total of 15 subjects were scanned. Because of individual tolerance to perform fixations without motion artifacts, it was not possible to scan both orbits of every subject, so some contributed data only for one orbit. Data was therefore obtained in 26 orbits with at least three horizontal gaze positions. In seven subjects who could perform longer data acquisition, MRI was done in 4 to 6 gaze directions, which permitted linear regression of morphometric parameters against gaze angle in individual subjects. These individual linear regressions compare effects of gaze within the same orbits of the same individuals, and so avoid interindividual variability.

Digital MRI images were quantified using both the imaging program (ImageJ64; provided in the public domain by W. Rasband, National Institutes of Health, Bethesda, MD, http://rsb.info.nih.gov/ij/, 1997–2009) and custom image analysis programs developed on statistical software (MATLAB; MathWorks, Boston, MA, 2011). Eye position in each gaze position was determined by the location of the optic nerve centroid relative to the orbital centroid at the globe-optic nerve junction.[16] Then, beginning as far posteriorly in each orbit as individual EOM bellies could be distinguished, each horizontal EOM was manually outlined and cropped in the imaging program (NIH) and saved as Tagged Image File Format (TIFF) files that included only the EOM belly (Fig. 1). Each TIFF file was then processed using statistical software (MathWorks) by automatically counting all the EOM pixels in the image file and converting those pixels into area in mm^2.

Three broad categories of morphometric parameters were determined for each subject in each gaze position: single plane measurements, partial volume measurements offset from the plane of maximum cross-section in central gaze, and partial volume measurements fixed with respect to the orbit. The single plane measurements included the change in EOM maximum cross-sectional area, the percent change in maximum cross-sectional area relative to central gaze, the maximum difference between cross-sectional areas in comparable image planes, the number of image planes by which the plane of maximum cross-sectional area shifted posteriorly, and the change in cross-sectional area one image plane posterior to the image plane of maximum cross-sectional area in central gaze.

The partial volumes were calculated by multiplying the EOM cross-sectional areas by the 2-mm slice thickness, then summing the in-plane volumes from contiguous image planes to create partial volumes that spanned the region of interest. The partial volume measurements offset from the plane of maximum cross-section in central gaze were based on the assumption that the largest change in EOM partial volume would include a shift of contracting EOM mass from this image plane posteriorly. These measurements included the partial volume change from central gaze of the two, three, and four image planes immediately posterior to the image plane containing the maximum cross-sectional area in central gaze.

The partial volume measurements fixed with respect to the orbit included two regions: the six contiguous image planes including and immediately posterior to the globe-optic nerve junction (midorbital region), and the four image planes beginning 14 mm posteriorly to the globe-optic nerve junction and continuing anteriorly (posterior orbital region). The midorbital region was selected as a region included in prior studies,[12,13] while the posterior orbital region included the most posterior image planes that were obtained in every subject.

The single plane and multiplane area and partial volume measurements were correlated with duction angle, with positive angles defined as duction toward an EOM's field of action and negative angles defined as duction away from that field of action. For example, for the medial rectus (MR), adduction was defined as positive and abduction as negative, while for the lateral rectus (LR), adduction was negative and abduction was positive.

Since EOM contractility is a physiologic behavior of every orbit, the individual orbit was considered the appropriate primary unit of analysis relevant to the questions under study.[17,18] In order to maximize statistical efficiency and avoid data loss, results of both orbits of volunteer subjects were included in linear regression analyses in cases where bilateral imaging could be performed in at least three gaze directions. This approach employs the entire available dataset, but includes variability from individual orbits and subjects. Significant findings from such analyses would therefore be strong, and directly applicable for comparison in other studies employing this common approach. Confirmatory linear regression analyses were performed within seven individual subjects in whom MRI could be performed 4 to 6 gaze positions for each orbit. This approach, which involves highly resource-intensive data collection, controls completely for individual variation among subjects, but necessarily yields a smaller dataset. It was not anticipated that either the pooled data or the individual subject approach would be differentially biased with respect to morphological indicators of EOM function under comparison.

Results

Imaging was performed bilaterally in 11 subjects, and unilaterally in four more subjects due to limitations on subject availability or endurance. A total of 101 MRI image sets were obtained for 26 orbits of 15 subjects, all in slightly varying gaze positions. Imaging included central gaze (taken as 0°) and at least one position of abduction and one position of adduction, while many orbits included multiple additional positions of abduction and adduction. Adduction ranged in magnitude from 4.8° to 32.9°, while abduction ranged from 7.1° to 27.2°.

All area and volume measures were highly statistically significantly correlated with duction angle ($P < 0.0001$ for all values), but not all correlations were equally strong. The coefficients of determinations R^2, which represent the fraction of variance accountable by duction angle, are summarized in the Table. The best single plane correlation with duction angle was the maximum difference in cross-sectional areas between any image planes at the same anatomic location in the orbit, for which $R^2 = 0.92$ for the MR and 0.91 for the LR. This calculation, however, required prior knowledge of whether the EOM was contracting or relaxing in the measured field of gaze. If the EOM was contracting (e.g., the MR during adduction), the greatest positive difference in cross-sectional areas between corresponding image planes from central to eccentric gaze was used to define the measure, while if the EOM was relaxing (e.g., the MR during abduction), the greatest negative difference was selected. This measure, which requires a priori knowledge, would not be useful in detecting abnormal or unexpected contractility. Instead, the best single plane measure to detect contraction or relaxation was the percent change in maximum cross-sectional area, for which $R^2 = 0.79$ for MR and 0.78 for LR (Fig. 2). The anteroposterior movement of the image plane of maximum cross-sectional area was the single-plane measure that had the poorest correlation with degrees of duction, $R^2 = 0.44$ for MR and $R^2 = 0.52$ for LR.

While it is recognized that total EOM volume is conserved regardless of gaze angle, partial volume measures in midorbit can reflect shifts in EOM volume distribution that would also diminish the potential effect of fluctuations in measured EOM cross-sections due to nerve and vascular entries and other sources of anatomical "noise" in single image planes. Partial volume measures all had robust correlations with duction angle. There was a monotonic increase in the coefficient of determination when the number of image planes used to calculate the posterior partial volume was increased from two to three to four (Table). The strongest correlation was for the change in partial volume for the four image planes immediately posterior to the plane containing the maximum EOM cross-section in central gaze. This measure was not obtained in all subjects; however, because this measurement occasionally required very posterior image planes that were not included in the imaging range in every subject. Instead, posterior orbital partial volumes were available in all subjects and provided almost as strong a correlation, especially when combined with the measured change in posterior orbital partial volume of the antagonist EOM (Fig. 3). The combined agonist/antagonist posterior partial volumes provided the highest coefficient of determination of any functional measure, $R^2 = 0.95$ for the MR and LR combined.

The foregoing data were obtained in 26 orbits in which MRI were obtained in at least three gaze directions to evaluate group effects. This dataset reflected variation among individual subjects, as well as effects of duction angle. For the 13 orbits with imaging sets available in four, five, or six different positions of horizontal gaze, there were sufficient measurements that individual linear regressions could be performed within subjects, so that each regression reflected duction angle only. In eight orbits, an MRI was obtained in central gaze and at least two adducted and two abducted positions. Not surprisingly, since this individual subject regression approach avoids confounding by interindividual anatomical variability, correlations within subjects were much stronger than for the data pooled for multiple individuals. The intrasubject coefficient of determination R^2 for combined agonist/antagonist changes in posterior partial volume exceeded 0.97 for all seven subjects (range 0.97–0.99, Fig. 4). Similar trends held for most of the other single plane and partial volume measurements, with the exception of movement of the plane of maximum cross-sectional area. In five subjects at least one MR, and in six subjects at least one LR, exhibited an identical 2- or 4-mm change in plane of max cross-section regardless of duction. This resulted in a poor correlation of location of plane of

Table. Correlation of Change in Areas and Volumes with Duction Angle (Deg)

	Coefficient of Determination R^2	
Measure	Medial Rectus	Lateral Rectus
Single plane measures		
Change in maximum area	0.79	0.77
Percent change in maximum area	0.79	0.78
Maximum difference	0.92	0.91
Movement of image plane	0.44	0.52
Change in area 2 mm posterior	0.69	0.75
Partial volume offset from plane of max cross-section		
2 planes posterior	0.89	0.86
3 planes posterior	0.93	0.88
4 planes posterior	0.94	0.90
Fixed orbital partial volumes		
Mid-orbit	0.74	0.51
Posterior orbit	0.88	0.89
Posterior agonist/antagonist	0.95	0.95

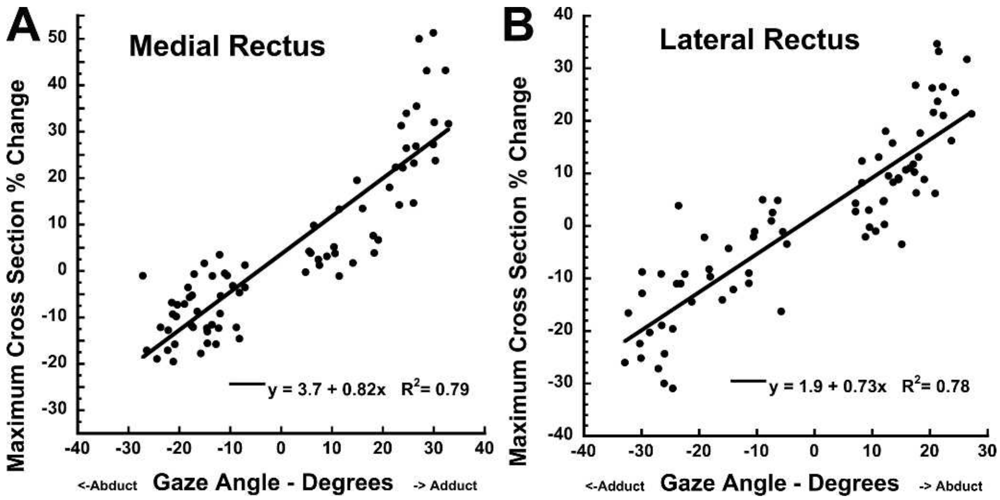

FIGURE 2. Scatter plots demonstrating the relationship of the percentage change in maximum cross-sectional area with degrees of horizontal duction. (A) Medial rectus. (B) Lateral rectus. These muscles had similar linear regressions and coefficients of determination R^2. Data from 26 orbits of 15 subjects.

maximum cross-section with duction angle, and a large spread of values for the correlation determination, $R^2 = 0.15$ to 0.97.

DISCUSSION

Functional imaging has become a powerful tool in the study of the nervous system. While most studies of the skeletal motor system have been able to employ direct measures of force or electromyographic activity, studies of the ocular motor system have typically been limited to gaze angle. As has been earlier emphasized by Miller,[19] there are many circumstances where gaze angle is overdetermined in relationship to the mechanical states of the actuating EOMs: numerous combinations of coagonist and coantagonist cyclovertical EOM contractile states can be associated with the same gaze angle. It has been recently suggested that rectus EOMs consist of multiple compartments that may function differently in response to differing physiological situations such as ocular counter-rolling[20] and convergence.[21] It is thus important to develop functional measures of EOM contractility that might distinguish contributions from individual EOMs or compartments of individual EOMs. The current study examined multiple MRI measures of the functional contributions of horizontal rectus EOMs to horizontal duction, a situation in which the MR-LR antagonist pair makes the overwhelming contribution to duction. Both clinical experience with LR and MR paralysis and computational simulation[22] indicate that the vertical rectus and oblique EOMs contribute very little to horizontal duction.

The present data demonstrate that changes in MR and LR morphology are highly correlated with horizontal duction, and thus are highly correlated with contractility. The change in an EOM's maximum cross-sectional area demonstrates a strong

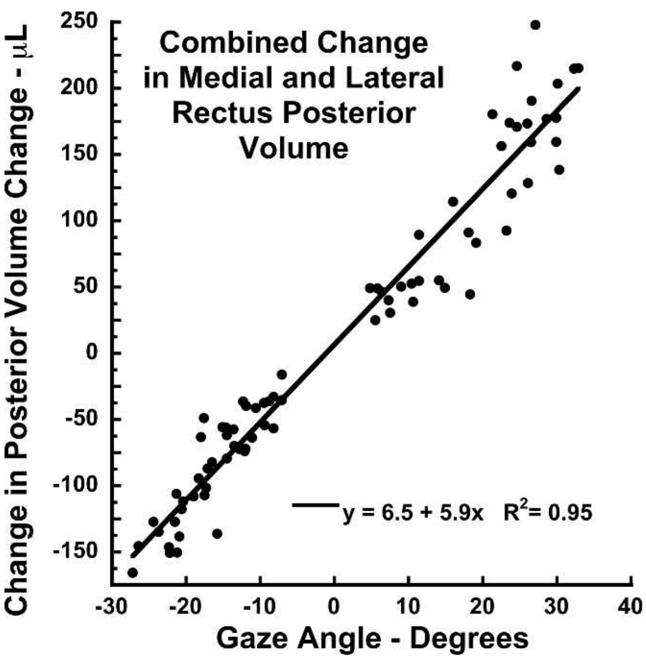

FIGURE 3. Scatter plot demonstrating the relationship of combined agonist/antagonist posterior partial volumes with horizontal duction. This measurement had the strongest correlation with degrees of duction for both horizontal rectus muscles. Data from 26 orbits of 15 subjects.

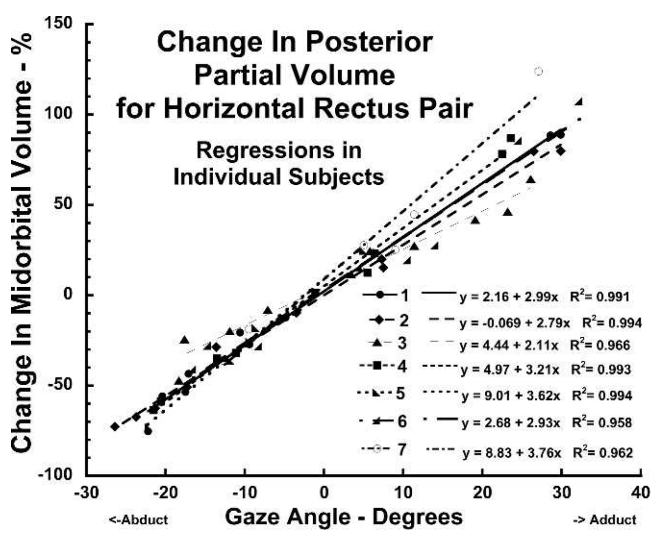

FIGURE 4. Percent change in posterior partial volume of the MR-LR antagonist pair as a function of horizontal duction. For each of the seven numbered subjects who achieved four to seven horizontal gaze positions per orbit, linear regression demonstrated excellent correlation with the magnitude of horizontal duction, accounting for 97% to 99% of the variance.

correlation with duction, with a contractile change of between 0.7% (LR) and 0.8% (MR) corresponding to each degree of duction (Fig. 2). We regard this measurement as the best single-plane measurement of horizontal rectus function, since it does not require prior knowledge of the EOM's contractile state. The anteroposterior movement of the image plane of maximum cross-sectional area had the weakest overall correlation. Probably because of the relatively low axial resolution of 2 mm corresponding to image plane thickness, movement of the image plane of maximum cross-section exhibited a threshold effect in some subjects. The image plane of maximum EOM cross-section does, on average, shift anteroposteriorly with gaze change, but the magnitude of the image plane displacement does not correlate as well with duction as the other measurements evaluated here. The location of maximum cross-section is therefore not a reliable quantitative measure of muscle function.

The posterior partial volume measurements had the best overall correlation with duction. The stronger correlation probably reflects the fusiform shape of the EOMs, and perhaps structural features in or around the lengths of the EOMs. During contraction, the entire posterior EOM belly thickened as the bulk of the EOM mass shifted posteriorly, and the multi-plane partial volume measurements capture that change in morphology better than single-plane measurements. Even among partial volume measurements, increasing the number of image planes from two to four resulted in a stepwise increase in the correlation coefficient (Table). The midorbital partial volumes had the weakest correlation among this group of measurements, probably because, in most subjects, this portion of the EOM included image planes anterior to the plane of maximum cross-sectional area. Those anterior image planes demonstrated a reduction in cross-sectional area during contraction and an increase in cross-sectional area during relaxation, offsetting the typical contractile changes seen further posterior in the orbit. The posterior partial volumes had a much stronger correlation with duction, and should be preferred over midorbital partial volume to detect and quantify EOM contractility.

The major limitation of this study, as with all MRI studies, is that EOM contractile force is not directly measured and correlated with the imaging changes in EOM morphology. Degrees of duction provides an estimate of the net contractile force in the agonist-antagonist pair, but it is likely that the contractile force required to rotate the globe may be nonlinear at the extremes of gaze, with proportionately greater force required to achieve maximum duction compared with smaller degrees of duction.

The other weakness of the study is that certain abnormal EOMs may not demonstrate the same contractile changes as these normal subjects. In patients with dysthyroid orbitopathy,[23] Duane syndrome,[6] congenital fibrosis syndromes,[12] and other clinical entities with abnormal EOMs, similar changes in EOM morphology on MRI may not accurately reflect the contractile forces being generated. More quantitative studies on the correlation of these measurements with duction are required before these results can be generalized to include those clinical conditions.

In summary, changes in EOM cross-sectional areas and posterior partial volumes are highly correlated with degrees of duction and thus contractility. Changes in single-plane maximum cross-sectional areas and posterior multiplane partial volumes can provide an accurate, quantitative estimate of EOM contractility, especially when the corresponding changes in the antagonist are included in the measurements.

References

1. Miller JM. Functional anatomy of normal human rectus muscles. *Vision Res*. 1989;29:223–240.
2. Demer JL, Kono R, Wright W. Magnetic resonance imaging of human extraocular muscles in convergence. *J Neurophysiol*. 2003;89:2072–2085.
3. Demer JL, Miller JM. Magnetic resonance imaging of the functional anatomy of the superior oblique muscle. *Invest Ophthalmol Vis Sci*. 1995;36:906–913.
4. Demer JL, Oh SY, Clark RA, Poukens V. Evidence for a pulley of the inferior oblique muscle. *Invest Ophthalmol Vis Sci*. 2003;44:3856–3865.
5. Demer JL, Miller JM, Koo EY, Rosenbaum AL. Quantitative magnetic resonance morphometry of extraocular muscles: a new diagnostic tool in paralytic strabismus. *J Pediatr Ophthalmol Strabismus*. 1994;31:177–188.
6. Demer JL, Clark RA, Lim KH, Engle EC. Magnetic resonance imaging evidence for widespread orbital dysinnervation in dominant Duane's retraction syndrome linked to the DURS2 locus. *Invest Ophthalmol Vis Sci*. 2007;48:194–202.
7. Demer JL, Clark RA, Lim KH, Engle EC. Magnetic resonance imaging of innervational and extraocular muscle abnormalities in Duane-radial ray syndrome. *Invest Ophthalmol Vis Sci*. 2007;48:5505–5511.
8. Demer JL, Miller MJ, Koo EY, Rosenbaum AL, Bateman JB. True versus masquerading superior oblique palsies: Muscle mechanisms revealed by magnetic resonance imaging. In: Lennerstrand G, ed. *Update on Strabismus and Pediatric Ophthalmology*. Boca Raton, FL: CRC Press; 1995:303–306.
9. Kushner BJ. Multiple mechanisms of extraocular muscle "overaction." *Arch Ophthalmol*. 2006;124:680–688.
10. Kushner BJ. Does extraocular muscle form denote function? *Arch Ophthalmol*. 2010;128:1604–1609.
11. Bloom JN, Graviss ER, Mardelli PG. A magnetic resonance imaging study of the upshoot-downshoot phenomenon of Duane's retraction syndrome. *Am J Ophthalmol*. 1991;111:548–554.
12. Demer JL, Clark RA, Engle EC. Magnetic resonance imaging evidence for widespread orbital dysinnervation in congenital fibrosis of extraocular muscles due to mutations in KIF21A. *Invest Ophthalmol Vis Sci*. 2005;46:530–539.
13. Clark RA, Demer JL. Enhanced vertical rectus contractility by magnetic resonance imaging in superior oblique palsy. *Arch Ophthalmol*. 2011;129:904–908.
14. Demer JL, Clark RA. Magnetic resonance imaging of human extraocular muscles during static ocular counter-rolling. *J Neurophysiol*. 2005;94:3292–3302.
15. Demer JL, Dusyanth A. T2 fast spin echo magnetic resonance imaging of extraocular muscles. *J AAPOS*. 2011;15:17–23.
16. Clark RA, Miller JM, Demer JL. Location and stability of rectus muscle pulleys inferred from muscle paths. *Invest Ophthalmol Vis Sci*. 1997;38:227–240.
17. Murdoch IE, Morris SS, Cousens SN. People and eyes: Statistical approaches in ophthalmology. *Br J Ophthalmol*. 1998;82:971–973.
18. Sainani K. The importance of accounting for correlated observations. *PM&R*. 2010;2:858–861.
19. Miller JM, Robins D. Extraocular muscle sideslip and orbital geometry in monkeys. *Vision Res*. 1987;27:381–392.
20. Clark RA, Demer JL. Differential lateral rectus compartmental contraction during ocular counter-rolling. *Inv Ophthalmol Vis Sci*. 2011;53:2887–2896.
21. Demer JL, Clark RA. Differential compartmental activity in lateral (LR) rectus during convergence: possible explanation of the force paradox? *Soc Neurosci Abstr*. 2011;699.604.
22. Demer JL. Extraocular Muscles. In: Tasman W, Jaeger EA, eds. *Duane's Clinical Ophthalmology*. Hagerstown, MD: Lippincott; 2009:1–30.
23. Ohnishi T, Noguchi S, Murakami N, et al. Extraocular muscles in Graves ophthalmopathy: usefulness of T2 relaxation time measurements. *Radiology*. 1994;190:857–862.